ELSEVIER

Journal of Chromatography A, 769 (1997) 59–69

JOURNAL OF CHROMATOGRAPHY A

Parameter estimation for the simulation of liquid chromatography

Ulf Altenhöner*, Markus Meurer, Jochen Strube, Henner Schmidt-Traub

Department of Chemical Engineering, University of Dortmund, 44221 Dortmund, Germany

Abstract

The simulation of preparative or production scale chromatographic processes becomes necessary, as far as not only separation but optimal operation is required. The proposed strategy for modelling and parameter estimation provides a straightforward method for successful imaging of chromatographic processes in computer mathematics as an axial dispersed tubular reactor model with linear diffusion between solid and mobile phase and arbitrary isotherms. Consistent data for parameter estimation are collected from a simple single-column setup. All calculations (parameter estimations and simulations) were performed using the dynamic simulation tool SPEEDUP (Aspen, Cambridge, MA, USA).

Keywords: Preparative chromatography; Computer simulation; Dynamic simulation; Parameter estimation; Adsorption isotherms; Mass transfer; Fructose; Glucose

1. Introduction

The precision of mathematical models describing the dynamic behaviour of chemical processes is seriously affected by errors in the determination of the various parameters. Chromatographic column models usually contain process parameters [flow-rate(s), feed concentration, temperature] imposed during operation and physicochemical parameters (dispersion coefficient, bed porosity, mass transfer coefficients, adsorption isotherms) whose values have to be previously estimated from experimental data. The former can be fixed and their real values are known with errors arising from the measurement instruments, the latter contain errors due to both the estimation procedure adopted to fit data and the experimental errors of the data itself [1]. To estimate the physicochemical or model parameters for chromatographic columns, several techniques have been developed in recent years as reviewed in Refs. [2] and [3]. Although the methods developed seem to deliver accurate figures, most attempts in modelling chromatographic processes yield only satisfactory but not good congruence of predicted and results found in experiments as shown in Ref. [2]. This statement becomes well understood, when considering how the used model parameters were gained: most of them are estimated from independent experiments with analytical mathematical methods derived from ideal models e.g., the elution by characteristic points method developed by Glueckauf [4]. The simulations using these parameters to calculate column behaviour are performed in a numerical way. On the way from experiment to simulated results three sources of error can be found: first, the experimental error, second, the simplifications resulting from the analytical parameter estimation and third, the numerical error of the simulation program. The experimental error depends on laboratory praxis and on the instruments used, so great efforts have to be made to reduce error. The other two sources of error can be eliminated easily by using the same mathematical tools for estimating and modelling. In this way the same simplifications are made for

*Corresponding author.

PII S0021-9673(97)00173-8

parameter estimation and calculations. Even the numerical error is the same. Hence if the model is capable of imaging the reality, good agreement of measurements and predictions can be expected.

This paper studies the modelling of a packed column using an ion-exchange resin as adsorbent and fructose and glucose as adsorbates. The experiments were performed on a preparative scale column, the simulations used SPEEDUP as the software platform.

2. Modelling of chromatographic columns

2.1. Model selection

As reviewed in Refs. [5] and [6] several different attempts have been made to create models for chromatographic columns. Van Deemter et al. presented a simple equilibrium stage model, calculating the height of every plate [7]. Other research workers developed stage models with mass transfer resistance and finally, dispersed plug flow models were designed using either lumped dispersion coefficients or explicit mass transfer equations. A full review is given in Ref. [18]. Although the stage models allow good fitting of experimental results for single components in linear chromatography, some problems evolve in their application for other systems. Katz et al. have shown [8], that peak dispersion and therefore HETP depends on the retention factor, even for linear isotherms. So the application of ideal stage models is only suitable when using different HETP for different components and changing HETP with concentration for nonlinear isotherms. Furthermore, plate models are not suitable for chromatographic units with changes in flow-rates [for example simulated moving-bed (SMB) technology) as shown in Refs. [9] and [10]. In this study, a dispersed plug flow model is used, thereby avoiding the inadequacies of the stage models.

2.2. Model equations

A mass balance is wrapped around a differential slice of the column, excluding the adsorbent particles. Convection and dispersion permeate the front ends of the volume element. Mass transfer to the adsorbent penetrates the solid–liquid interface contained in the volume èlement (Eq. (1)). Another balance is made around the particles (Eq. (2)). Homogenous concentration and instantaneous equilibrium inside the particles are assumed, so the concentration inside the pores of the particle $c_{p,j}$ is the same as the concentration on the outer surface. The overall mass transfer resistance is supposed to exist in the fluid film around the particle. This formulation of mass transfer kinetics is strictly valid for dominating mass transfer in the stagnant film or linear isotherms and negligible adsorption kinetics, which is true for most chromatographic systems as stated in Ref. [18] (p. 148). If diffusion in the pores is the limiting step and the isotherms show nonlinear behaviour, concentration differences (c_i) in Eqs. (1,2) should be replaced by the adsorbed concentrations (q_i). Finally, the adsorption isotherm links fluid and solid concentration (Eq. (3)).

$$\frac{\partial c_j}{\partial t} = -u_0 \cdot \frac{\partial c_j}{\partial x} + D_{ax} \cdot \frac{\partial^2 c_j}{\partial x^2} - k_{eff} \cdot \frac{6}{d_p} \cdot \frac{1-\epsilon}{\epsilon} \cdot (c_j - c_{p,j}) \quad (1)$$

$$\frac{\partial q_j}{\partial t} = k_{eff} \cdot \frac{6}{d_p} \cdot (c_j - c_{p,j}) \quad (2)$$

$$q_j = f(c_{p,j}, c_{p,h\neq j}, T) \quad (3)$$

This model is able to describe the dynamic behaviour of single chromatographic columns as well as that of more complicated systems like SMB [10] or closed-loop-recycle separation units. Furthermore, it is possible to implement any kind of adsorption isotherm described in algebraic equations, even the use of ion-exchange isotherms as described by Velayudhan and Horváth in Ref. [11] is possible. To solve the problem numerically, the partial differential equations are transferred into ordinary ones by the method of lines. As finite difference scheme in the axial direction, a formula proposed by Leonard [12] has been proved to be a robust, fast and accurate approximation. Danckwerts boundary conditions were used in a modified form [13]. For a column of 20 cm length about 4000 equations have to be calculated simultaneously.

2.3. Model parameters

It can be seen from Eqs. (1–3) that the mathematical description of the chromatographic column contains some model parameters to be estimated. These are the bed porosity ϵ and the axial dispersion coefficient D_{ax} describing the column and the packing behaviour, and the adsorption isotherms q (c) and the mass transfer coefficients k_{eff} characterising each solute and its interaction with the solid-phase. The particle diameter d_p is not considered as a model parameter, because it is always used in conjunction with k_{eff} in Eqs. (1,2) and therefore influencing the mass transfer only. This influence will be compensated by the estimation of the mass transfer coefficient, so all inaccuracies in the determination of d_p will be lumped into k_{eff}. The length and the diameter of the column are so called structure parameters, describing obvious characteristics of the chromatographic column.

The law of propagation of error states, that the imperfection of each parameter will contribute to the error of the result. Due to this, the accuracy of the simulation decreases with the number of parameters. This statement is in direct contrast to the observations resulting from peak fitting procedures, where each new parameter introduced enhances the accuracy of the model. The set of model parameters derived using this procedure are therefore "imperfect but consistent" and include the mathematical error hidden in the model.

According to these considerations, two contrary methods for parameter estimation can be described: the first attempts to find exact parameters but neglects interactions between them and the model therefore producing only a poor fit. The second ignoring physical facts but considering influences of the model and other parameters and in spite of this giving excellent fittings. Unfortunately, both kinds of parameter estimation strategies are unable to supply useful models for process optimization and design, because the former is not able to fit experimental data at all and due to the lack of a physicochemical background, the latter is not reliable for supporting changes of scale, flow-rate etc..

We suggest a feasible method to estimate a consistent set of parameters in an easy way by experiments performed in a single chromatographic column. Physical reasonability is granted by experimental design. The physicochemical model used to perform the simulation is also used to estimate the parameters. Therefore, the calculations are extremely reliable even for scale up experiments and deliver excellent accuracy.

2.3.1. Step 1: axial dispersion and bed porosity

The axial dispersion coefficient and the bed porosity are estimated from a pulse test of a non retained species. Similar experiments were performed for an analytical size column by Schneider and Hejtmanek [14].

The following analytical evaluation is presented to prove, that the experiment performed contains the desired information and allows the numerical calculation of the model parameters.

The bed voidage ϵ can be calculated from a characteristic time t_{char}, either the mean residence time, estimated from the first moment of the peak μ, or the time of the peak maximum t_{max} for symmetric peaks.

$$\epsilon = \frac{Q}{V_{total}} \cdot t_{char} \tag{4}$$

Where μ is evaluated by numerical integration of the peak data recorded:

$$\mu = \frac{\sum_{i=1}^{n} c_i \cdot t_i \cdot \Delta t_i}{\sum_{i=1}^{n} c_i \cdot \Delta t_i} \tag{5}$$

Lameloise and Viard proposed breakthrough curves for the measurement of external porosities and selected dextran as an excellent tracer for ion-exchange resins [15]. Unnecessary effort is caused by the performance of breakthrough curves, because no improvement in the accuracy of the estimated bed porosities can be reached. The number of measurements recorded in the significant time remains constant for pulse and breakthrough curve, because both have the same length in the time domain for the case of a non retained component. Therefore no additive data can be recorded.

Axial dispersion coefficients can be estimated from the Van Deemter equation.

$$\mathrm{HETP} = A + \frac{B}{u_0} + Cu_0 \tag{6}$$

$$A = 2\gamma_2 d_p \tag{7}$$

where

$$B = 2\gamma_1 D_M \tag{8}$$

For a non adsorbable component, C as a mass transfer characteristic becomes zero and the Van Deemter equation reduces to (Eq. (9)):

$$\mathrm{HETP} = A + \frac{B}{u_0} \tag{9}$$

Ruthven proposes in [5] the Eq. (10) for the calculation of the axial dispersion coefficient

$$D_{ax} = \gamma_1 D_M + \gamma_2 d_p u_0 \tag{10}$$

Insertion of Eqs. (7,8) into Eq. (10) yields

$$D_{ax} = \left(A + \frac{B}{u_0}\right) \cdot \frac{u_0}{2} \tag{11}$$

and combined with Eq. (9)

$$D_{ax} = \mathrm{HETP} \cdot \frac{u_0}{2} \tag{12}$$

The HETP can then be easily estimated from an eluted peak by using the first moment μ and the second σ.

$$\mathrm{HETP} = \frac{\sigma^2}{\mu^2} \cdot L \tag{13}$$

The second moment can be calculated from the recorded data in a numerical way:

$$\sigma^2 = \frac{\sum_{i=1}^{n} c_i (t_i - \mu)^2 \Delta t_i}{\sum_{i=1}^{n} c_i \Delta t_i} \tag{14}$$

Although these theoretical reflections seem to promise good results, parameter estimation performed using simulations can be more beneficial. Back mixing volumes, if present, can be easily estimated and errors can be instantly detected by comparing experimental and computed plots.

2.3.2. Step 2: adsorption isotherms and mass transfer coefficients

Several proposals have been made to estimate adsorption isotherms. An extended discussion on this topic has been given by Guiochon et al. [18]. Only a few methods are suitable for the determination of multicomponent isotherms: the competitive frontal analysis, the pulse method, the simple wave method, the computation of elution profiles as presented here, and the static method. The static method cannot assure consistency of data, because it is performed offline of the chromatographic set. Pulse methods often use radioactive substances, assume linear behaviour and require a lot of solvent for high concentrations. Frontal analysis and the simple wave method cannot be distinguished by experimental design but only by the mathematic methods used. For the experiments presented here, experiments similar to frontal analysis in baseline mode were performed. As a first approximation of the adsorption isotherms the basic equations of frontal analysis were used together with numerical integration of the chromatographic plot.

The integral balance wrapped around the column from the time of injection (t_{inj}) to the time when the concentration plateau is reached at the end of the column (t_∞) yields:

$$\epsilon V(c_j^{II} - c_j^{I}) + (1 - \epsilon)V(q_j^{II} - q_j^{I}) = Q \int_{t_{inj}}^{t_\infty} (c_j^{II} - c_j(t))\mathrm{d}t \tag{15}$$

Applying this at each concentration step, one point of the isotherm can be estimated. In contrast to the characteristic point techniques, frontal analysis does not use the shape of the breakthrough curve for any calculations, so that the shape of the curve contains information about the isotherm, axial dispersion and adsorption or mass transfer resistance. As long as the axial dispersion coefficient is estimated as described above and a good guess of the isotherm is given by Eq. (15), fitting of a computed elution profile to the

curve will provide the kinetics as well as corrections to the proposed isotherm.

3. Experimental

The experimental setup is presented in Fig. 1.

3.1. Chemicals

Distilled water was used as solvent. The chemicals were Dextran, M_r 200 000–300 000, clinical grade (ICN Biochemicals, Cleveland, OH, USA), glucose, analytical-reagent grade and fructose, analytical-reagent grade (Merck, Darmstadt, Germany). For high concentration experiments refined juices of fructose and glucose were kindly provided by Südzucker (Mannheim, Germany).

3.2. Column

The experiments were performed on a jacketed glass column (500×44 mm, Amicon, Germany) with variable column lengths. The column heads were adjusted to 211 mm distance. The ion-exchange resin used was Imac HP 1320 in Ca-form kindly provided by Rohm and Haas (Frankfurt, Germany). This resin is a gel-type ion-exchanger. The particles are ideal spheres, mean particle diameter was found to be 0.325 mm by optical (Carl Zeiss, Wetzlar, Germany) and laser optical particle size analysis (Microtrax X 100). The diameter distribution is very small. The product specifications provide for an average particle size of 0.320 mm.

3.3. Instruments

The liquids were stored in stainless steel tanks. All tanks were stirred and temperature controlled. The liquid was delivered by a two piston pump (Sykam, Gilching, Germany), capable of pumping up to 300 ml/min. The flow of the pump was permanently displayed by either a coriolis flowmeter (K2, ABB Industrietechnik, Meerbusch, Germany) or a graduated measuring glass. The fluids were degassed in a laboratory-made vacuum degasser (vacuum pump by Leybold, Hanau, Germany, 80 PTFE tubes in parallel each 3 m long) before entering the pump. An injection valve with variable loop volume (Rheodyne, Cotati, CA, USA) was installed downstream of the pump for sample injection. A single tube heat exchanger (laboratory-made, PTFE) was installed to control the temperature of the fluid entering the column by adjusting the shell side temperature of the heat exchanger.

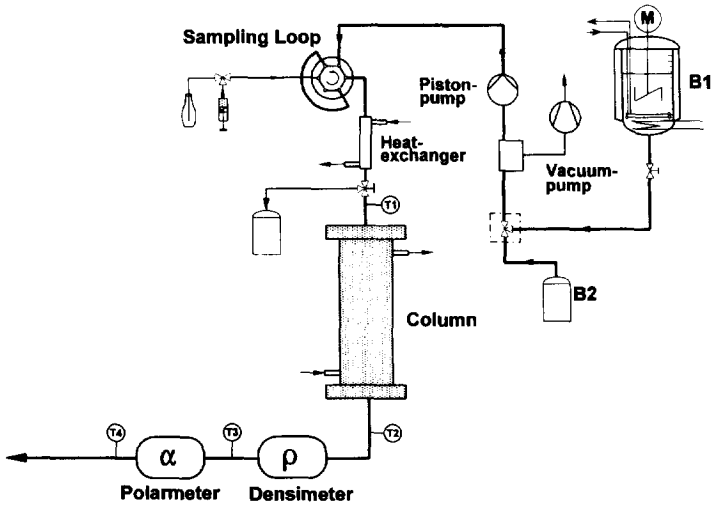

Fig. 1. Experimental setup.

3.4. Detectors and data acquisition

Concentrations were detected with an *u*-tube densimeter (500×2 mm tube, Centec, Bruchköbel, Germany) and a polarimeter (IBZ Messtechnik, Hannover, Germany). Both were calibrated for fructose and glucose at various concentrations and temperatures, allowing calculation of the concentrations of each species even when no separation was achieved. Temperatures were measured with thermocouples inserted before and after the column and the polarimeter. Data was recorded on a personal computer using laboratory-made software (written in Visual Basic; Microsoft). The data files were uploaded to a SUN Ultrasparc which performed the SPEEDUP calculations.

4. Results and discussion

4.1. Bed porosity and axial dispersion

In preliminary experiments, three substances were tested as nonadsorbable tracers Dextran II (M_r 5–40·10^6), Dextran I (M_r 200 000–300 000) and calciumchloride. Only Dextran I was found to be a suitable tracer. Calcium chloride showed a dependence of residence time on peak concentration, while Dextran II eluted in asymmetric peaks. To estimate the residence time distribution of the experimental setup independently of the packed bed, column heads were mounted face to face and the elution of a peak was recorded. It was found that the time constant as well as band broadening were small compared to that of the packed bed.

Experiments were performed at different flow-rates (10–90 ml/min) and different temperatures (50 and 70°C). The results are presented as a function of the Reynolds number Re_p.

$$Re_p = \frac{u_0 d_p}{\nu} \tag{16}$$

In Fig. 2 HETP versus Re_p is presented. This modification of the Van Deemter plot allows to compare fluids of different viscosities, here caused by different temperatures. Despite of a wide range of flow-rates, no significant minimum was found. This implies that neither mass transfer nor axial diffusion are dominating, leading to the conclusion that Dextran I is not, or only weakly, adsorbed.

Figs. 3 and 4 display the measured bed porosity as a function of Reynolds number. Surprisingly porosity was not found to be constant but to increase with growing Reynolds number. Various interpretations can be found for this behaviour. First of all, adsorption can be excluded because it would cause the opposite effect and retention would be enhanced at slow flow-rates. Transport phenomena (like film diffusion) can also be excluded, causing only

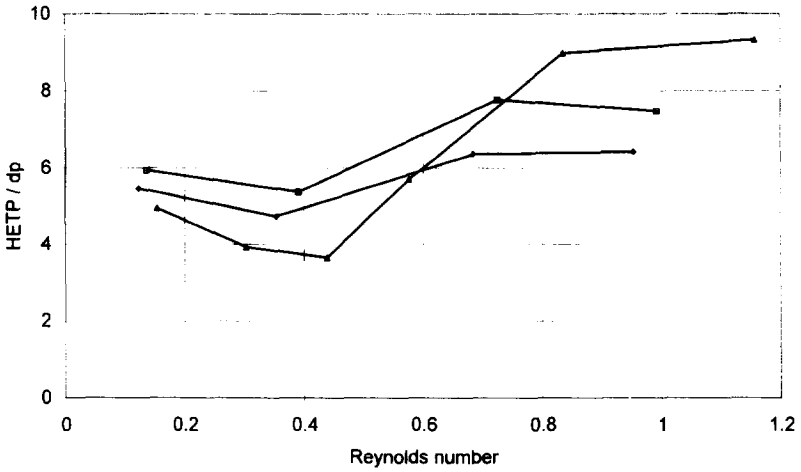

Fig. 2. HETP versus Reynolds number (□ 70°C, first row; △ 70°C, second row; ◇ 50°C).

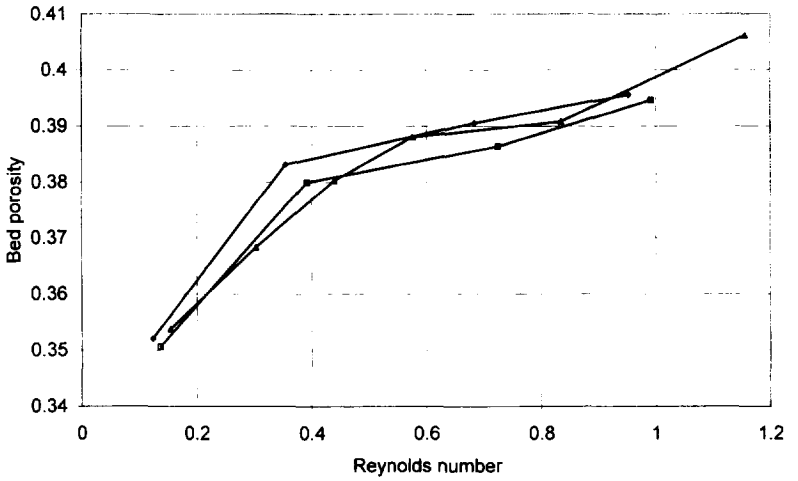

Fig. 3. Bed porosity calculated from peak maximum time (□ 70°C, first row; △ 70°C, second row; ◇ 50°C).

changes in residence time distribution but not affecting the mean residence time itself [16]. The elastic properties of the experimental setup can be named as one reason for the growing void volume, namely the compression of the soft gel particles and the deformation of the plastic column heads caused by high pressure drops. Alternatively clusters, which are frequented neither by diffusion nor by convection at low flow-rates but penetrated by fast moving liquid, may exist in the packed bed. Although the response function of the measure instruments contribute to this effect. First of all the preparative cells used are quite large (1.5 ml for the densimeter). Therefore only average concentrations in the cells are measured. The delivery of data from the measure instruments is delayed by the electronics in the instruments themselves, using averaging to stabilise the signals. This delayed signals are recorded with the system time of the PC used for data acquisition as time axis. Therefore time and signal are not exactly matching. For low flow-rates the volume of the cell will dominate the delay. For higher velocities averaging in the electronics will become dominant.

The numbers estimated by using the peak maxi-

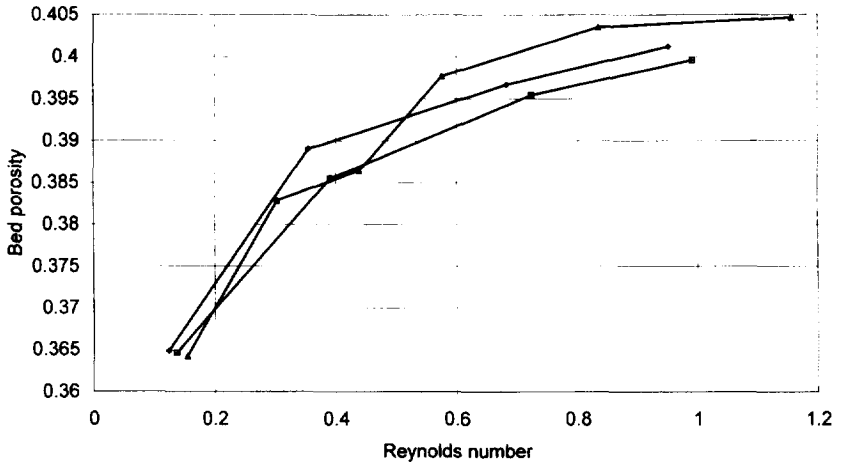

Fig. 4. Bed porosity calculated from mean residence time (□ 70°C, first row; △ 70°C, second row; ◇ 50°C).

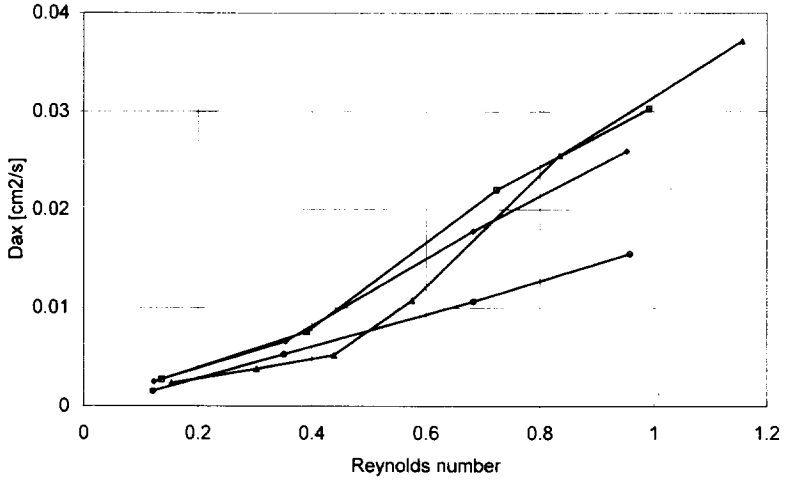

Fig. 5. Dispersion coefficient versus Reynolds number (□ 70°C, first row; △ 70°C, second row; ◇ 50°C;○ Fan and Wen [17]).

mum time and the mean residence time differ slightly, hence the peaks found are not quite symmetric. This may arise partly from a back-mixing volume at the end of or after the column, for example the detector cell itself.

The estimated figures for the axial dispersion coefficient are presented in Fig. 5.

Fan and Wen proposed a widely used correlation for axial dispersion coefficients using dimensionless characteristic numbers [17].

$$Bo = \frac{0.2}{\epsilon} + \frac{0.011}{\epsilon} \cdot (\epsilon Re_p)^{0.48} \quad (17)$$

where

$$Bo = \frac{u_0 d_p}{D_{ax}} \quad (18)$$

Good conformity is found for Reynolds numbers smaller then 0.5. For higher fluid velocities, estimated values are bigger than those calculated; here the validity of the empirical correlation of Fan and Wen seems to be exceeded.

4.2. Adsorption isotherms

Adsorption isotherms were estimated for glucose, fructose and mixtures of both at three different temperatures (39, 49 and 59°C). This temperature

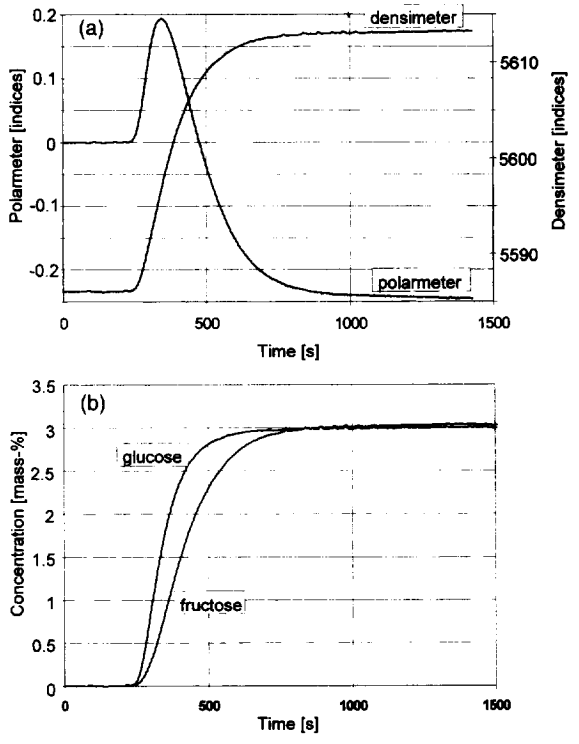

Fig. 6. (a) Breakthrough curve of fructose and glucose (fructose 3 %, m/m; glucose 3 %, m/m; flow 30 ml/min; temperature 59°C). (b) Concentration plot of the breakthrough curve (fructose 3 %, m/m; glucose 3 %, m/m; flow 30 ml/min; temperature 59°C).

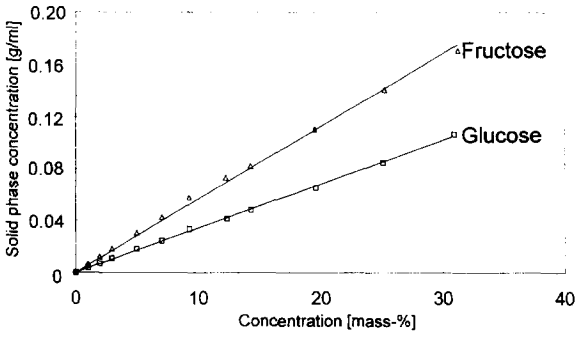

Fig. 7. Isotherms for fructose and glucose at 39°C ($q_{1,\text{fructose}} = 0.005634 c_{\text{fructose}}$, $q_{\text{glucose}} = 0.003401 c_{\text{glucose}}$).

range was selected because the separation of different anomers caused by mutarotation was found in previous studies in analytical columns especially for glucose within this range [19].

The chromatogram for the breakthrough curve of a mixture of fructose and glucose is represented in Fig. 6a.

The peak which can be seen at the curve of the polarimeter is the change in the composition of the eluted mixture, changing from the positive turning glucose to the negative turning fructose. Using the calibration of the measure instruments the concentration plot can be generated (Fig. 6b).

Isotherms of the pure species and mixtures with concentrations up to 30%, m/m were estimated based on several experiments. Fig. 7 depicts the isotherms for both pure components at a temperature of 39°C. Both isotherms are linear, yielding a constant separation factor of 1.66.

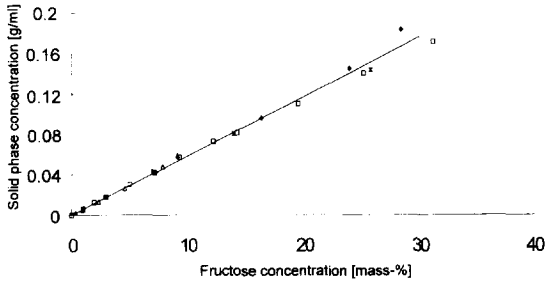

Fig. 9. Isotherm of fructose in the presence of glucose (□ pure glucose; * $f:g$ ratio = 3:1; △ $f:g$ ratio = 1:1; ♦ $f:g$ ratio = 1:3).

Increasing the temperature reduces the slope of the isotherms for both species as expected from thermodynamical considerations. This effect is more marked with fructose, the more strongly adsorbed component (see Fig. 8). This indicates that separation factors will decline with rising temperatures.

Isotherms for the mixtures were determined at a constant ratio of both components. Fructose as the more strongly adsorbed component was not influenced by the presence of glucose and can simply be described with a linear isotherm (Fig. 9).

Conversely fructose decreases the adsorption of glucose as can be seen in Fig. 10.

An isotherm equation similar to the well known multicomponent Langmuir attempt was found to fit the data (Eq. (19)).

$$q_G = 0.04 \cdot \frac{0.085 c_G}{1 + 0.065 c_F^{0.8} + 0.01 c_F} \tag{19}$$

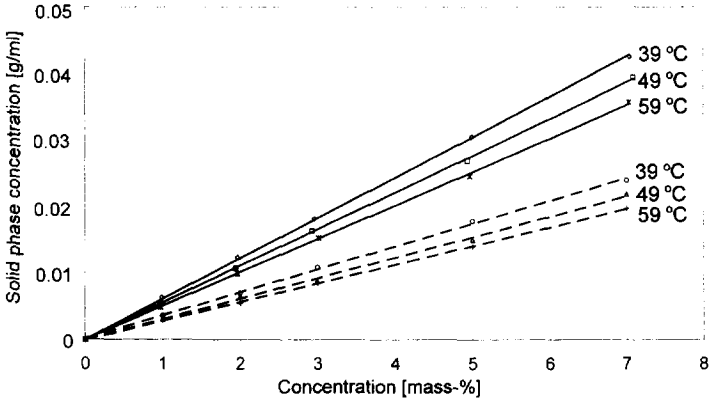

Fig. 8. Isotherms for fructose (———) and glucose (– – –) at different temperatures.

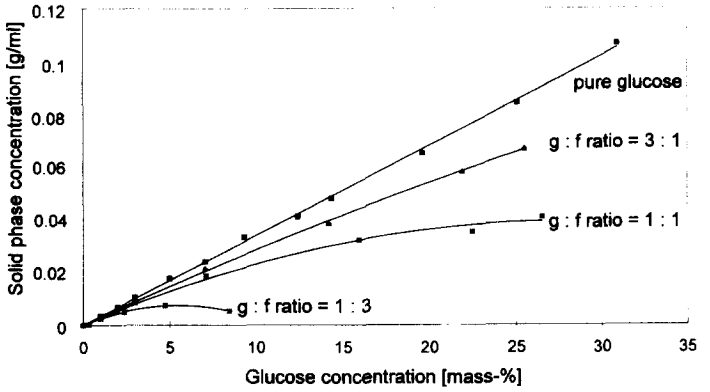

Fig. 10. Isotherm of glucose in the presence of fructose.

This equation provides an excellent fit except for glucose to fructose ratios above 1: 3.

Fig. 11 depicts the comparison between a predicted and a measured desorption curve for fructose at 30%, mm. Parameters used for the calculation were estimated from different experiments as described above. Congruence is quiet satisfying. At the beginning of the desorption the measured results show a steeper slope as the calculated. At the end it is the opposite way. Further examinations have to be done for the elucidation of this behaviour. It may be contributed to backmixing in the experimental setup or nonlinear mass transfer.

5. Conclusion

A straightforward method for the estimation of model parameters for the simulation of liquid chromatography columns has been developed and proved. Unfortunately experiments could only be presented for linear isotherm although there is no restriction in the model to linear cases. The experimental effort can be reduced to a minimum. In the experimental setup, a new combination of sensors has demonstrated its ability to determine the concentrations of mixtures only differing by the rotation of light, e.g., enantiomers.

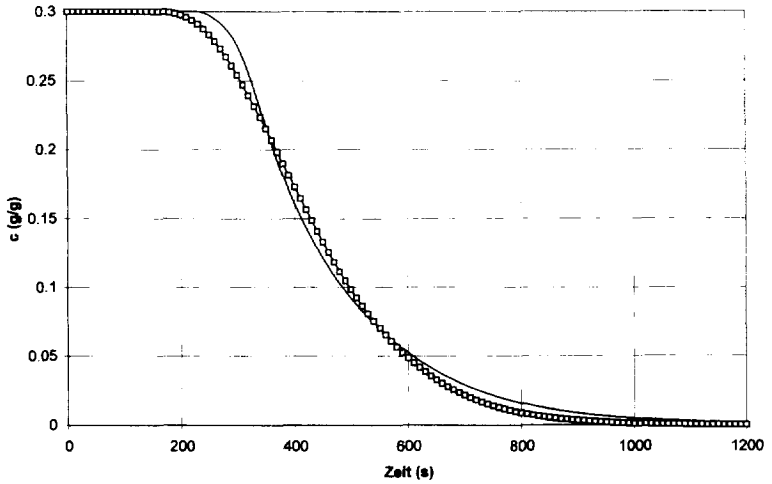

Fig. 11. Predicted (□) and measured (———) desorption curve for fructose, $T=39°C$, flow=31.02 ml/min, $L=21.28$ cm, $d=4.4$ cm. "Zeit" = time.

6. Symbols

A	first parameter of the van Deemter equation
B	second parameter of the van Deemter equation
Bo	Bodenstein number
C	third parameter of the van Deemter equation
c_F	concentration of fructose in the bulk phase
c_G	concentration of glucose in the bulk phase
c_i	concentration at time step number i
c_j	concentration of species j in the bulk phase
$c_{p,j}$	concentration of species j on the surface of the particle
D_{ax}	axial dispersion coefficient
D_M	molecular diffusivity in the fluid
d_p	particle diameter
d	diameter of the column
HETP	height equivalent a theoretical plate
k_{eff}	effective mass transfer coefficient
L	length of the column
n	number of volume elements
Q	volume flow
q_G	solid-phase concentration of glucose
q_j	solid-phase concentration of species j
Re_p	Reynolds number
T	temperature
t	time
t_{char}	characteristic time
t_i	time of time step i
t_{max}	residence time of the peak maximum
u_0	interstitial velocity
V_{total}	column volume
V	volume
x	axial coordinate in the column

6.1. Greek symbols

γ_1	statistic packing factor
γ_2	labyrinth factor
Δt_i	length of time step i
ϵ	bed porosity
μ	mean residence time
σ	standard deviation
υ	viscosity

References

[1] O. Paladino, M. Ratto and P. Costa, Chem. Eng. Sci., 50 (1995) 3829–3822.

[2] A. Seidel-Morgenstern, Mathematische Modellierung der präparativen Flüssigchromatographie, Deutscher Universitäts Verlag, Berlin, 1995.

[3] P. Schneider and V. Hejtmanek, Chem. Eng. Sci., 48 (1993) 1163–2268.

[4] E. Glueckauf, Nature, 156 (1945) 748.

[5] D.M. Ruthven, Principles of Adsorption and Adsorption Processes, Wiley, New York, 1984.

[6] D.M. Ruthven and C.B. Ching, in P. Ganetsos and P.E. Barker (Editors), Modeling of Chromatographic Processes Preparative and Production Scale Chromatography, Marcel Dekker, New York, 1993.

[7] J.J. Van Deemter, F.J. Zuiderweg and A. Klinkenberg, Chem. Eng. Sci., 5 (1956) 271.

[8] E. Katz, K.L. Logan and R.P.W. Scott, J. Chromatogr., 170 (1983) 51–75.

[9] H. Schmidt-Traub, J. Strube, H.-I. Paul and S. Michel, Chem.-Ing.-Tech., 67 (1995) 323–326.

[10] J. Strube and H. Schmidt-Traub, Computers Chem. Eng., 20 Suppl. (1996) S641–646.

[11] A. Velayudhan and Cs. Horváth, J. Chromatogr. A, 663 (1994) 1–10.

[12] B.P. Leonard, Comp. Meth. Appl. Mech. Eng., 19 (1979) 59–98.

[13] P.V. Danckwerts, Chem. Eng. Sci., 2 (1953) 1–13.

[14] P. Schneider and V. Hejtmanek, Chem. Eng. Sci., 48 (1993) 1163–1168.

[15] M.-L. Lameloise and V. Viard, J. Chromatogr. A, 679 (1994) 255–259.

[16] L.G. Gibilaro, Chem. Eng. Sci., 33 (1987) 487–492.

[17] L.T. Fan and C.Y. Wen, Models for Flow Systems and Chemical Reactors, Marcel Dekker, New York, 1975.

[18] G. Guichon, S.G. Shirazi and A.M. Katti, Fundamentals of Preparative and Nonlinear Chromatography, Academic Press, Boston, MA, 1994.

[19] C. Buttersack, W. Wach and K. Buchholz, in J. Weitkamp, H.G. Karge, H. Pfeifer and W. Hölderich (Editors), Zeolites and Related Microporous Materials: State of the Art 1994 (Studies in Surface Science and Catalysis, Vol. 84, Part B, Elsevier, Amsterdam, 1994, pp. 1363–1371.